Advanced Composite Materials
Publication details, including instructions for authors and subscription information:
http://www.tandfonline.com/loi/tacm20

Effect of Microstructure and Silicon Carbide on the Elevated Temperature Properties of Multi-layer Spray Deposition Al-8.5Fe-1.3V-1.7Si/SiCP Composite

Yiqiang He [a] , Zhengkun Xu [b] , Lichao Feng [c] , Jinsong Chen [d] , Feng Shang [e] , Hua Chen [f] & Zhen-Hua Chen [g]

[a] College of Mechanical Engineering, Huaihai Institute of Technology, Lianyungang 222005, People's Republic of China; College of Materials Science and Engineering, Hunan University, Changsha, Hunan 410082, People's Republic of China;, Email: ant210@126.com

[b] Department of Mechanical Engineering, Zhangjiajie Institute of Aviation Industry vocational, Zhangjiajie, Hunan 427000, People's Republic of China

[c] College of Mechanical Engineering, Huaihai Institute of Technology, Lianyungang 222005, People's Republic of China

[d] College of Mechanical Engineering, Huaihai Institute of Technology, Lianyungang 222005, People's Republic of China

[e] College of Mechanical Engineering, Huaihai Institute of Technology, Lianyungang 222005, People's Republic of China

[f] College of Mechanical Engineering, Huaihai Institute of Technology, Lianyungang 222005, People's Republic of China

[g] College of Materials Science and Engineering, Hunan University, Changsha, Hunan 410082, People's Republic of China

To cite this article: Yiqiang He , Zhengkun Xu , Lichao Feng , Jinsong Chen , Feng Shang , Hua Chen & Zhen-Hua Chen (2011): Effect of Microstructure and Silicon Carbide on the Elevated Temperature Properties of Multi-layer Spray Deposition Al-8.5Fe-1.3V-1.7Si/SiCP Composite, Advanced Composite Materials, 20:2, 169-178

To link to this article: http://dx.doi.org/10.1163/092430410X539271

///VSP///

Advanced Composite Materials 20 (2011) 169–178

ADVANCED COMPOSITE MATERIALS
brill.nl/acm

Effect of Microstructure and Silicon Carbide on the Elevated Temperature Properties of Multi-layer Spray Deposition Al–8.5Fe–1.3V–1.7Si/SiC$_P$ Composite

Yiqiang He [a,c,*], **Zhengkun Xu** [b], **Lichao Feng** [a], **Jinsong Chen** [a], **Feng Shang** [a], **Hua Chen** [a] **and Zhen-hua Chen** [c]

[a] College of Mechanical Engineering, Huaihai Institute of Technology, Lianyungang 222005, People's Republic of China
[b] Department of Mechanical Engineering, Zhangjiajie Institute of Aviation Industry vocational, Zhangjiajie, Hunan 427000, People's Republic of China
[c] College of Materials Science and Engineering, Hunan University, Changsha, Hunan 410082, People's Republic of China

Received 9 June 2009; accepted 20 July 2010

Abstract

Multi-layer spray deposited Al–8.5Fe–1.3V–1.7Si alloy was co-deposited with 15 vol% SiC particulate (SiC$_P$). The microstructure of the composite as-rolled has been determined using transmission electron microscopy (TEM). Elevated temperature properties of the composite have been investigated by comparing the tensile mechanical properties at 20°C, 315°C and 400°C for the composite. The significance of these results for microstructure at elevated temperature, operating strengthening mechanisms and the effects of SiC$_P$ reinforcement in such an alloy system, is discussed.

Keywords

Multi-layer spray deposition, elevated temperature properties, SiC reinforcement, microstructure, Al–8.5Fe–1.3V–1.7Si/SiC$_P$ composite

1. Introduction

The combination of multi-layer spray deposition and reinforcement with co-deposited ceramic particulate is a powerful tool for developing high performance materials with enhanced strength and stiffness, wear resistance, stability of properties at elevated temperature and reduced density. The Al–Fe–V–Si alloy system has attracted considerable interest in recent years due to its high-temperature appli-

---

[*] To whom correspondence should be addressed. E-mail: ant210@126.com
Edited by JSCM and KSCM

DOI:10.1163/092430410X539271

cations. In recent years, there has been a large amount of research on the rapidly solidified Al–Fe–V–Si alloys for possible applications in aerospace structures [1–7], especially on the multi-layer spray deposited Al–Fe–V–Si alloy. The Al–8.5Fe–1.3V–1.7Si (8009 type) alloy is believed to be a promising candidate for application at elevated temperatures, especially if it is reinforced with ceramic particulates (for example, SiC particulates), short fibers or whiskers [8–12]. These composites possess good elevated-temperature properties and high creep strength due to the high fraction (typically 20–30%) of stable dispersoids (viz. $Al_{12}(Fe, V)_3Si$ dispersoids) which, owing to their low coarsening rate, maintain their strengthening role also for long exposures at elevated temperature [13]. Furthermore, such ceramic particulate reinforcements increase their Young's modulus at least to about 700 K [14].

Considerable research effort [9, 11, 15] has been expended in the development of semi-empirical approaches and analytical treatments for a description of creep behavior of Al–Fe–V–Si alloy or SiC/Al–Fe–V–Si composite. However, few investigations of the elevated temperature properties of SiC reinforced aluminum alloys matrix composite have been reported. This article shows the results of an elevated temperature properties study on multi-layer spray deposition Al–8.5Fe–1.3V–1.7Si/SiC_P composite. The elevated temperature properties data are combined with data on the effect of microstructure and silicon carbide.

2. Materials and Experimental Method

The material used in this study was multi-layer spray deposited Al–8.5 wt%Fe–1.3 wt%V–1.7 wt%Si (namely 8009Al) with 15 vol% α-SiC particulates. The composite preforms were first fabricated by a self-developed spray deposition apparatus. The processing parameters of the spray deposition experiments are given in Table 1. Hot extruding was used for densification of the composite preforms. For hot extruding processing, the composite billets were heated up to 490°C and kept for an hour and then extruded into a sheet of 125 mm in width and 20 mm in thickness at an extrusion ratio λ of 11. The as-extruded composites were rolled at 490°C. The obtained Al–8.5Fe–1.3V–1.7Si/SiC_P composite sheets were 0.6–0.8 mm in thickness.

Table 1.
Process parameters of the spray deposition experiments

Process parameters	Value
Atomization temperature (K)	1223–1373
Diameter of the melt stream (mm)	3.2–3.6
Spray height (mm)	200–350
Rotate speed of the substrate ($r{\cdot}min^{-1}$)	100–350
Scan velocity of the nozzle (s)	10–30
Pressure of the atomization gas (MPa)	0.7–0.9

Constant strain rate of 0.2 mm/min tensile tests were performed using an electromechanical testing machine at temperatures of 20, 315 and 400°C. The microstructure of the composite was analyzed by means of X-ray diffraction (XRD), optical microscopy (OM), scan electron microscopy (SEM) and transmission electron microscopy (TEM).

3. Results

3.1. Microstructure

Transmission electron microscopy (TEM) showed relatively uniform distributions of the silicides ($Al_{12}(Fe, V)_3Si$) in the α-Al matrix in either unreinforced or reinforced samples, and optical microscopy (OM) showed relatively uniform distribution of the SiC_P in the reinforced sample.

Compact and uniform microstructure can be seen both in the Al–8.5Fe–1.3V–1.7Si alloy unreinforced (Fig. 1(a)) and in the Al–8.5Fe–1.3V–1.7Si alloy reinforced with SiC particles (Fig. 1(c)). The composite showed a random distribution of SiC_P, of size 8 to 12 μm (Fig. 1(c)) with occasional evidence of smaller shattered SiC particles with size about 3 μm. The presence of pores around the SiC particles and between deposited particles gives rise to poor mechanical properties due to oxide films and insufficient metallurgical bonding. Typical TEM micrographs of the silicides ($Al_{12}(Fe, V)_3Si$) in the α-Al matrix in unreinforced alloy are shownare in Fig. 1(b), in which silicides of 500 nm in diameter can be seen. TEM micrographs of the silicides ($Al_{12}(Fe, V)_3Si$) in the α-Al matrix in the as-spray deposited, as-extruded, and as-rolled after extruding condition shown in Fig. 1(d), (e) and (f) respectively, which are dominated by a generally uniform distribution of nearly spherical silicide particles with most at grain boundaries and a few at within α-Al grains. With extruding following multi-layer spray deposition, α-Al grains grow to a certain extent, from about 300 nm in size to about 600 nm in size, whereas, with rolling following, grain size decreases to 400 nm. Matrix grain size was not measured easily in Fig. 1(f), because grain boundaries were harder to distinguish because of high dislocation density and high SiC content. As indicated in Fig. 1(d), (e) and (f), all silicides ($Al_{12}(Fe, V)_3Si$) size of reinforced alloy remained stable at 50 to 80 nm.

Comparing Fig. 1(b) with Fig. 1(d), (e) and (f), it may be observed that with the reinforcement of SiC particulates, silicide particle size decreases to a great extent (from 500 nm to 50 nm) because of the increase of the cooling rate of α-Al matrix. At the same time, grain size decreases also.

Considering the effect of SiC particle addition on the microstructure of alloy matrix, it is necessary to determine the microstructures of the SiC–matrix interface. Figure 2(a) shows the morphology the distribution of the dispersoids, and the size is about 50 nm. An amorphous SiC–Al interface of about 5 nm in width is found in the composite as shown in Fig. 2(b). Nano-crystal cells can be seen from Fig. 2(c), which formed into a transition region (200–400 nm in width) near the SiC particle

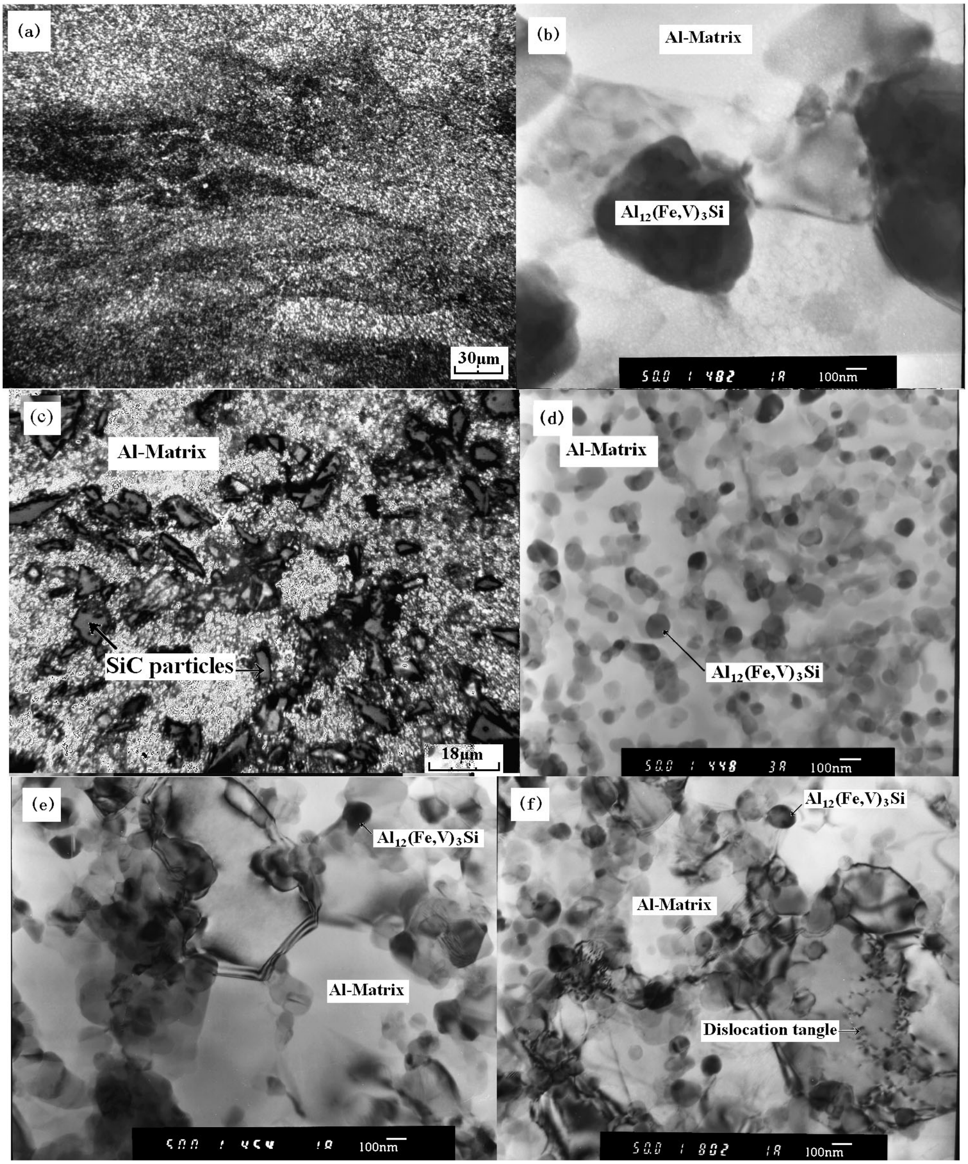

Figure 1. Micrographs of unreinforced (a) and reinforced (b), (c), (d), (e) Al–8.5Fe–1.3V–1.7Si alloy, TEM micrographs (a)–(d), showing uniform distributions of silicides ($Al_{12}(Fe, V)_3Si$) in the α-Al matrix and OM micrograph, (e) showing uniform distribution of SiC_P; (a) unreinforced alloy as-rolled after extruding, (b) reinforced alloy as-spray deposited, (c) reinforced alloy as-extruded, (d) reinforced alloy as-rolled after extruding, (e) SiC in reinforced alloy.

boundary in the matrix. The interface between the SiC particle and the Al matrix is the SiC contact with Al matrix, as illustrated in Fig. 2(d) and 2(e). As shown in Fig. 2(d), some rod-like Al_4C_3 phase between the SiC particles and the matrix was

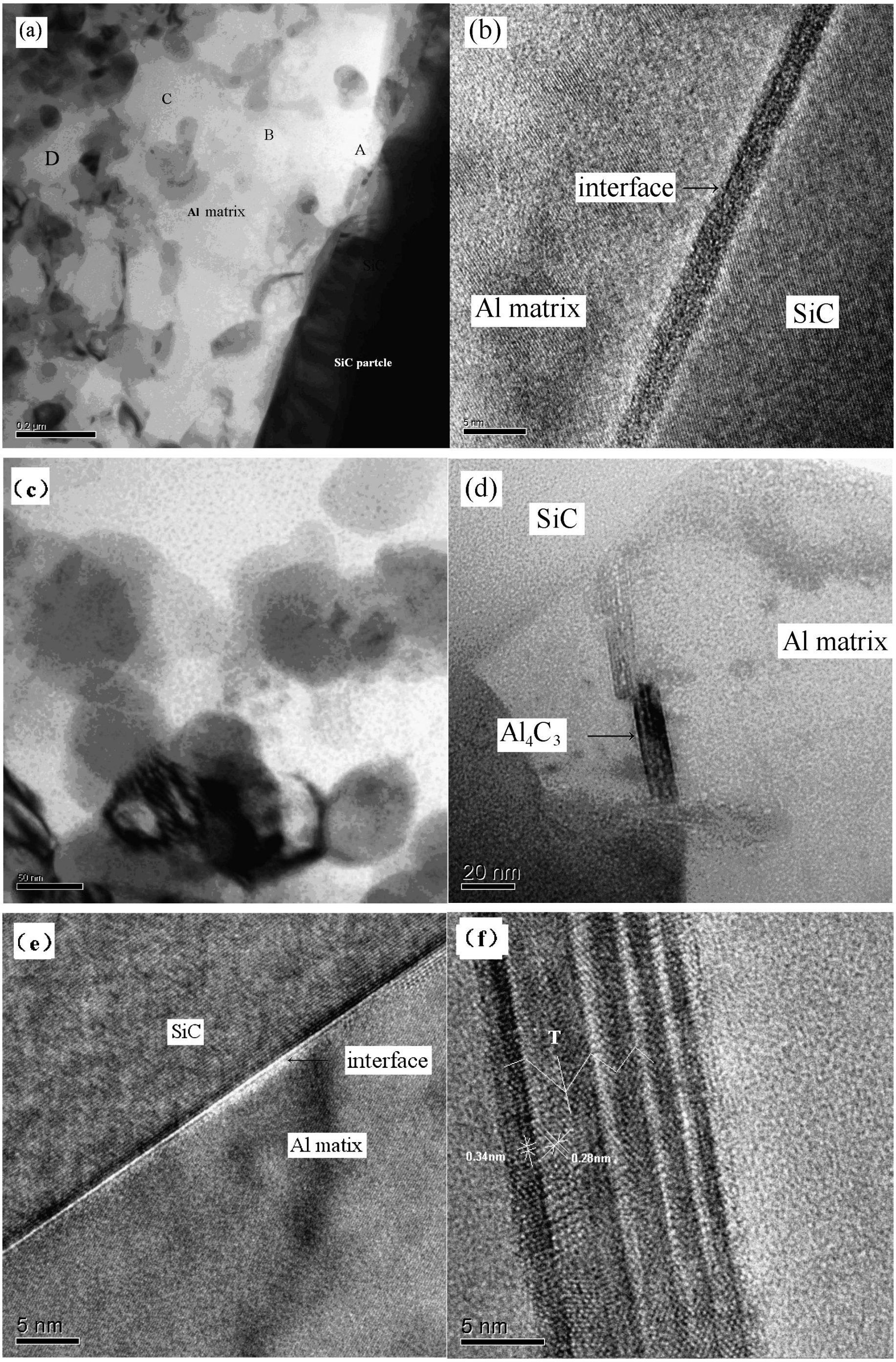

Figure 2. HRTEM micrographs of the SiC–matrix interface in the as-rolled Al–8.5Fe–1.3V–1.7Si/15SiC$_P$. (a) Al matrix and SiC particle, (b) amorphous SiC–matrix interface, (c) area near the interface in matrix, (d), (e) interface of crystallographic orientation relationships, and (f) Al_4C_3.

Table 2.
Si concentration at different points in matrix in Fig. 2(a) near the SiC–matrix interface

Position	A	B	C	D
Si concentration (at%)	30.13	28.39	25.32	21.22

detected, which was about 10 nm in diameter and 50 nm in length in the matrix near the interface. It can be considered harmless to the interface bonding strength since it was of quite small dimension. Furthermore, a clean, smooth and uniform interface was observed between the SiC particles and the Al matrix in Fig. 2(e). The Al_4C_3 phase was derived from the reaction between aluminum and SiC. This reaction originates from a dissolution–precipitation mechanism [16]. SiC is dissolved in Al, resulting in the saturation of carbon in Al, and precipitation of Al_4C_3 in the form of tabular aggregates which penetrate the SiC. It can be concluded that diffusion bonding results in a strong interfacial bonding in the composite. It should also be pointed out that some kinds of crystallographic orientation relationships may exist between the SiC particles and the Al matrix as shown in Fig. 2(e), and the atomic match bonding is possibly the reason for the high interface bonding strength in the spray-deposited composite. Figure 2(f) is a TEM image of the Al_4C_3 phase with high magnification in Fig. 2(d). As seen from Fig. 2(f), the Al_4C_3 phase exhibits the micro-twin microstructure. The twinned Al_4C_3 phases belong to the hexagonal system, which is a 180° secondary rotation twin with (003) plane as twinning plane and [001] direction as twinning axis. The long axis direction of Al_4C_3 is parallel to (003) plane and perpendicular to the [001] direction. The long axis direction of Al_4C_3 is the [210] direction. The Al_4C_3 phases are 180° secondary rotation twins with (003) plane as twinning plane and [001] direction as twinning axis [17].

Table 2 shows the obvious silicon concentration gradient in the matrix near the SiC–matrix interface. The silicon concentration fell from 30.13 at% at point A to 21.22 at% at point D in Fig. 2(a), which means partial dissolution of the SiC particle surface and interface reaction between the SiC particles and alloy matrix.

3.2. Mechanical Properties

The tensile properties at 20, 315 and 400°C given in Table 3 show ultimate and proof strengths decreasing with increase in test temperature, whether unreinforced or reinforced. In contrast, elongations to fracture for both increase to some extent with test temperature increase. Reinforcement increases ultimate tensile strength by 13 at% to 20 at% for Al–8.5Fe–1.3V–1.7Si at 20, 315 and 400°C while elongation to fracture was reduce at all test temperatures. Ultimate tensile strengths of Al–8.5Fe–1.3V–1.7Si at 315°C (with or without reinforcement) remain up to about 55% of values measured at 20°C, while the ones for both reinforced and unreinforced are typically one-third of their strengths on testing at 20°C. With SiC

Table 3.
Tensile properties at 20, 315 and 400°C*

Condition	Al–8.5 wt%Fe–1.3 wt%V–1.7 wt%Si	
	Unreinforced	+15 vol%SiCP
Tested at 20°C		
UTS (MPa)	470	535
$\sigma_{0.2}$ (MPa)	470	485
ε_F (%)	4	2.5
E (GPa)	88	107
Tested at 315°C		
UTS (MPa)	250 ± 4	300 ± 5
$\sigma_{0.2}$ (MPa)	200 ± 3	245 ± 4
ε_F (%)	7	5.5
Tested at 400°C		
UTS (MPa)	165 ± 5	186 ± 5
$\sigma_{0.2}$ (MPa)	130	150
ε_F (%)	9	7.5

* Where UTS = ultimate tensile strength; $\sigma_{0.2} = 0.2\%$ proof stress; ε_F = elongation to fracture.

particle addition, the Young's modulus of the alloy increased from 88 GPa to about 107 GPa.

4. Discussion

4.1. Microstructure

The larger silicide particulate size of ~500 nm for Al–8.5Fe–1.3V–1.7Si alloy without reinforcement compared with ~80 nm for the alloy reinforced with SiC particulates reflects both a relatively coarse scale of microstructure in the as-rolled after extruding Al–8.5Fe–1.3V–1.7Si alloy and appreciable coarsening of the silicide associated with processing at a relatively high temperature (495°C). The Al–Fe–V–Si silicide ($Al_{12}(Fe, V)_3Si$) dispersoid size of ~80 nm of reinforced alloy is similar to that reported by previous workers for consolidated Al–Fe–V–Si [18–20]. In the first instance, the presence of SiC_P elevates the cooling rate to 10^4–10^6 K/s, which contributes to a much finer scale of microstructure (including grains of α-Al matrix and silicide particles). In the next instance, it is attributed to that the fact that the silicides deposited in the processing of spray deposition tend to cluster and grow up at grain boundaries at a relatively high temperature in the next processing. The silicides will decompose and transform to coarse phase of $Al_{13}Fe_4$ of exposure at a high temperature for a long time. The absence of the $Al_{13}Fe_4$ and stabilization of the silicide ($Al_{12}(Fe, V)_3Si$) in the SiC_P-reinforced composite could be attributed to partial dissolution of SiC_P, injecting silicon into the matrix; this would tend to stabilize the Al–Fe–V–Si silicide ($Al_{12}(Fe, V)_3Si$) against its replacement by embrittling $Al_{13}Fe_4$. Such partial dissolution of SiC_P could also account for the precipitation of Al_4C_3 which appears in the investigation of Hambleton *et al.* [21]; it thus provides indirect supporting evidence for the observed stabilization for Al–Fe–V–Si silicide ($Al_{12}(Fe, V)_3Si$) in the presence of SiC_P.

4.2. Mechanical Properties

The more excellent mechanical properties for Al–Fe–V–Si alloy reinforced with SiC particulates compared with the unreinforced alloy at all the three test temperatures brings about this improvement through the operation of several factors.

The presence of the SiC particles improved the strength mainly by the load transfer from the matrix to the reinforcement due to the mismatch in the elastic constants. SiC particles and α-Al matrix bond together compactly through shear deformation. As well known, the strength of SiC particles is higher than that of the α-Al matrix, which resulted in a stagnant zone of high dislocation density near the SiC particle. Besides, the subsequent hot working (extrusion, rolling) of blunt SiC particles with a wedge angle increased the strength of the composite.

Aluminum matrix composites have been widely studied since it was found that ceramic whisker or particulates could greatly increase the specific modulus and other mechanical properties of such aluminum alloys. The addition of SiC particulates to aluminum alloys increased the moduli by about 30%, but the high temperature strength of the composite, primarily controlled by the composition and heat treatment of the aluminum alloy matrix, is not promising. It was concluded that the enhancement of the high temperature strength was dominated by the microstructure of the matrix, but also was affected by addition of SiC particulates. As previously mentioned, the adding of SiC_P elevates the cooling rate of the matrix greatly; this contributes to a much finer scale of microstructure of the matrix (including grains and silicide dispersions), and stabilizes the Al–Fe–V–Si silicide ($Al_{12}(Fe, V)_3Si$) against its replacement by embrittling $Al_{13}Fe_4$, both of which contribute to the excellent high temperature mechanical properties. The clean, smooth and uniform interface of crystallographic orientation relationships existing between the SiC and Al matrix results in a high strength bond at the interface between the SiC particle and the Al matrix in the composite, and contributes to the excellent mechanical properties.

Fine Al_4C_3 particles were dispersed in the Al matrix, strengthening the composite through precipitation strengthening [22, 23], which improves the mechanical properties of the composite further.

5. Conclusions

1. Mechanical properties of SiC_P/Al–8.5Fe–1.3V–1.7Si composite are greatly improved when compared with that of Al–8.5Fe–1.3V–1.7Si alloy without SiC particle reinforcement at ambient temperature, which results from the much

finer microstructure (grains and dispersed particulates) of the composite as a result of the adding of SiC particles.

2. The addition of SiC particulates to aluminum alloys could greatly increase the modulus of aluminum alloys, and the indirectly evaluated high temperature strength to a certain extent.
3. The adding of SiC_P elevates the cooling rate of the matrix greatly, which contributes to a much finer scale of microstructure of the matrix, and stabilizes the Al–Fe–V–Si silicide ($Al_{12}(Fe, V)_3Si$) against its replacement by embrittling $Al_{13}Fe_4$, both of which contribute to the excellent high temperature mechanical properties.
4. The clean interface of crystallographic orientation relationships results in a high strength bond. Both of the strong bond interfaces contribute to improve the mechanical properties. Some rod-like Al_4C_3 phase of about 10 nm in diameter and 50 nm in length is distributed in the matrix near the interface. Fine twinned Al_4C_3 phases are dispersed in the Al matrix: these strengthen the composite by precipitation strengthening and improve the mechanical properties of the composite further.

Acknowledgements

The research described in this publication was made possible by financial support of the Natural Science Foundation of China (No. 51004050), Talent Introduction Foundation of Huaihai Insititute of Technology (KQ09028) and Natural Science Foundation of Jiangsu Colleges and Universities (No. 09KJD430001).

We would like to acknowledge the contribution of Prof. Dr. Gang Chen to this project and for his wonderful guidance and supervision so that we could improve the quality of this report.

Other special thanks are given to Prof. Hongge Yan, Mr. Liang Hao, and Mr. Xianjue Yin from Hunan University for their patience throughout the process of writing this report.

Finally, we wish to express the thanks and appreciation to the people who have contributed to this dissertation.

References

1. D. J. Skinner, R. L. Bye, D. Raybould and A. M. Brown, Dispersion strengthened Al–Fe–V–Si alloys, *Scripta Metall.* **20**, 867–872 (1986).
2. K. S. Ravichandran and E. S. Darakadasa, Advanced Aerospace Al Alloys, *J. Metals* **39**, 28–32 (1987).
3. D. J. Chellman, J. C. Ekvall and R. A. Rainen, Elevated temperature PM aluminum alloy for aircraft structure, *Metall. Powder Rep.* **43**, 672–674 (1988).
4. Y.-W. Kim, Advanced aluminum alloys for high temperature structural applications, *Industrial Heating* **55**, 31–34 (1988).

5. F. H. Fones, Dispersion strengthened aluminum alloys, *Metall. Powder Rep.* **43**, 342–348 (1988).
6. P. S. Gilman and S. K. Das, Rapidly solidified aluminum alloys for high temperature/high stiffness application, *Metall. Powder Rep.* **44**, 616–620 (1989).
7. F. H. Froes, W. E. Quist and S. K. Das, Advanced lightweight metals using rapid solidification, *Metall. Powder Rep.* **43**, 392–404 (1989).
8. F. Carreño, G. Gonzáles-Doncel and O. A. Ruano, High temperature deformation behavior of an Al–Fe–V–Si alloy, *Mater. Sci. Engng: Struct. Mater.: Prop. Microstruct. Proc.* **A164**, 216–219 (1993).
9. S. J. Zhu, L. M. Peng, Z. Y. Ma, J. Bi, F. G. Wang and Z. G. Wang, High temperature creep behavior of SiC whisker-reinforced Al–Fe–V–Si composite, *Mater. Sci. Engng* **A215**, 120–124 (1996).
10. F. Carreño and O. A. Ruano, Separated contribution of particles and matrix on the creep behavior of dispersion strengthened materials, *Acta Mater.* **46**, 159–167 (1998).
11. L. M. Peng, S. J. Zhu, Z. Y. Ma, J. Bi, F. G. Wang, H. R. Chen and D. O. Northwood, High temperature creep deformation of $Al_{18}B_4O_{33}$ whisker-reinforced 8009 Al composite, *Mater. Sci. Engng* **A265**, 63–70 (1999).
12. Z. Y. Ma and S. C. Tjong, High-temperature creep behavior of SiC particulate reinforced Al–Fe–V–Si alloy composite, *Mater. Sci. Engng A: Struct. Mater.: Prop. Microstruct. Proc.* **278**, 5–15 (2000).
13. S. Spigarelli, Interpretation of creep behaviour of dispersion-strengthened Al–Fe–V–Si alloys in terms of detachment mechanisms: an overview, *Mater. Sci. Engng* **A337**, 306–314 (2002).
14. D. J. Lloyd, Particle reinforced aluminium and magnesium matrix composites, *Intl Mater. Rev.* **39**, 1–23 (1994).
15. J. Čadek, K. Kuchařová and S. J. Zhu, High temperature creep behaviour of an Al–8.5Fe–1.3V–1.7Si alloy reinforced with silicon carbide particulates, *Mater. Sci. Engng* **A283**, 172–180 (2000).
16. L. Cao, L. Geng, C. K. Yao and T. C. Lei, Interface in silicon carbide whisker reinforced aluminum composites, *Scripta Metall.* **23**, 227–230 (1989).
17. J. C. Romero and R. J. Arsenault, Anomalous penetration of Al into SiC, *Acta Metall. Mater.* **43**, 849–857 (1995).
18. D. J. Skinner and K. Okazaki, High strength Al–Fe–V alloys at elevated temperatures produced by rapid quenching from the melt, *Scripta Metall.* **18**, 905–909 (1984).
19. S. Hariprasad, S. M. L. Sastry and K. L. Jerina, Deformation behavior of a rapidly solidified fine grained Al–8.5%Fe–1.2%V–1.7%Si alloy, *Acta Metall. Mater.* **44**, 383–389 (1996).
20. R. E. Franck and J. A. Hawk, Effect of very high temperatures on the mechanical properties of Al–Fe–V–Si alloy, *Scripta Metall.* **23**, 113–118 (1989).
21. R. Hambleton, H. Jones and W. M. Rainforth, Effect of alloy composition and reinforcement with silicon carbide on the microstructure and mechanical properties of three silicide dispersion strengthened aluminium alloys, *Mater. Sci. Engng* **A304–306**, 524–528 (2001).
22. V. Garibay-Febles, H. A. Calderon and F. C. Robles-Hernández, Production and characterization of (Al, Fe)–C (graphite or fullerene) composites prepared by mechanical alloying, *Mater. Manuf. Proc.* **15**, 547–576 (2000).
23. J.-C. Lee, H.-K. Seok and H.-I. Lee, Alloy design of thixoformable wrought SiC/Al alloy composites, *Mater. Res. Bull.* **34**, 35–42 (1999).